

TRANSITION VELOCITY FUNCTION FOR IMPULSE CONTROL SYSTEMS

Stephen van Duin¹, Matthias Ahlswede² and Christopher D. Cook¹

¹ Faculty of Engineering, University of Wollongong, Northfields Avenue, Gwynnville, Australia

² Institute of Production Engineering and Machine Tools, Leibniz University Hannover, Hannover, Germany

Keywords: Impulsive Control, Static Friction, Limit Cycle, Stick-slip, Impulse Shape, Friction Model, Accuracy.

Abstract: This paper presents a modified impulse controller that is used to improve the velocity tracking of a servomechanism having characteristics of high nonlinear friction. A hybrid control scheme consisting of a conventional PID part and an impulsive part is used as a basis to the modified controller. This has previously been used to improve the position and velocity tracking of robot manipulators at very low velocities. Experiments show that at higher velocities the improved performance of the impulse part of the hybrid controller diminishes and can be counterproductive at these speeds when compared to conventional PID control alone. The modified hybrid impulse controller in this paper uses a mathematical function to transition the amount of torque from an impulse as a function of velocity to achieve more precise tracking across a range of velocities.

1 INTRODUCTION

Precision robot manufacturers continually strive to increase the accuracy of their machinery in order to remain competitive. The ability of a robot manipulator to position its tool centre point to within a very high accuracy allows the robot to be used for more precise tasks. For positioning of a tool centre point, the mechanical axes of a robot will be required to be precisely controlled around zero velocity where friction is highly non-linear and difficult to control. Furthermore, precise velocity control at high velocities is typically required for increased productivity. Each axis of a robot is typically controlled by a servomechanism and this paper deals with improving the control of these basic robot components in the presence of friction.

Nonlinear friction is inherently present in all mechanisms and can cause stick-slip during precise positioning. In many instances, stick-slip has been reduced or avoided by modifying the mechanical properties of the system; however this approach may not always be practical or cost effective. Alternatively, advances in digital technology have made it possible for the power electronics of servomechanisms to be controlled with much greater

flexibility. By developing better controllers, the unfavourable effects of non-linear friction may be reduced or eliminated completely.

Impulse control has been successfully used for accurate positioning of servomechanisms with high friction where conventional control schemes alone have difficulty in approaching zero steady state error. Static and Coulomb friction can cause a conventional PID controller having integral action (I), to overshoot and limit cycle around the reference position. This is particularly a problem near zero velocities where friction is highly non linear and the servomechanism is most likely to stick-slip. Despite the above difficulties, PID controllers are still widely used in manufacturing industries because of their relative simplicity and reasonable robustness to parameter uncertainty and unknown disturbances.

Stick-slip can be reduced or eliminated by using impulsive control near or at zero velocities. The impulsive controller is used to overcome static friction by impacting the mechanism and moving it by microscopic amounts. By combining the impulsive controller and conventional controller the PID part can be used to provide stability. Moving towards the reference position the impulse controller is used to improve accuracy for the final positioning where the error signal is small.

By applying a short impulse of sufficient force, plastic deformation occurs between the asperities of mating surfaces resulting in permanent controlled movement. If the initial pulse causes insufficient movement, the impulsive controller produces additional pulses until the position error is reduced to a minimum.

A number of investigators have devised impulsive controllers which achieve precise motion in the presence of friction by controlling the height or width of a pulse. Yang and Tomizuka (Yang et al., 1988) applied a standard rectangular shaped pulse in which the height of the pulse was a force 3 to 4 times greater than the static friction to guarantee movement. The width of the pulse was adaptively adjusted proportional to the error and was used to control the amount of energy required to move the mechanism towards the reference position. Alternatively, Popovic (Popovic et al., 2000) described a fuzzy logic pulse controller that determined both the optimum pulse amplitude and pulse width simultaneously using a set of membership functions. Hojjat and Higuchi (Hojjat et al., 1991) limited the pulse width to a fixed duration of 1ms and varied the amplitude by applying a force about 10 times the static friction.

In a survey of friction controllers by Armstrong-Hélouvy (Armstrong- Hélouvy et al., 1994), it is commented that underlying the functioning of these impulsive controllers is the requirement for the mechanism to be in the stuck or stationary position before subsequent impulses are applied. Thus, previous impulse controllers required each small impacting pulse to be followed by an open loop slide ending in a complete stop.

van Duin (van Duin et al., 2006), used a hybrid PID + Impulsive controller to improve the precision of a robot manipulator arm in the presence of static and Coulomb friction. The design and functioning of the controller does not require the mechanism to come to rest between subsequent pulses, making it suitable for both point-to-point positioning and speed regulation. van Duin (van Duin et al., 2006) manipulated the pulse shape to match the dynamic friction by making this shape responsive to very small changes in velocity.

The error in positioning during different tracking tasks at zero and low velocities was greatly improved. However, further experiments showed that the PID + Impulse controller had greater errors at high velocities compared to a simple PID controller alone.

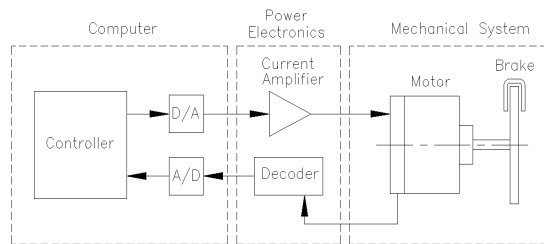


Figure 1: Experimental friction test bed.

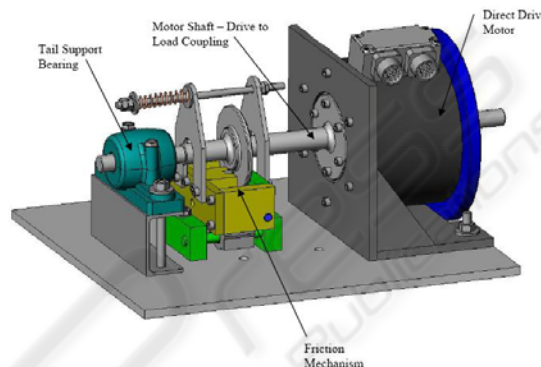


Figure 2: Three dimensional drawing of the friction test bed.

This paper presents a modified impulsive controller where the impulsive part of the hybrid PID + Impulse controller is gradually disabled at higher velocities so that the conventional linear PID part is eventually solely providing the driving torque. It is shown that at greater velocities, the static and Coulomb friction is less influential and that the system is more dominated by the relatively linear viscous frictional effects. Using a transition function the performance is shown to be improved for both low and high velocities, while maintaining system stability.

2 EXPERIMENTAL SYSTEM

2.1 Servomechanism

For these experiments a purpose built single axis friction test-bed was used to simulate the conditions typically observed in an industrial robot arm.

Figures 1 and 2 show the experimental friction test bed system that consists of a single axis direct drive servomechanism actuator coupled to a friction generating disk brake. Torque is transmitted by the actuator to the friction mechanism through a direct coupled shaft to eliminate the presence of backlash, gear cogging, belt cogging etc. Direct drive isolates

the friction characteristics; however, the impulse control systems in this paper have been repeated on a Hirata ARi350 SCARA robot with comparable results.

Position data is obtained from a shaft encoder housed within the motor and has a maximum resolution of 2^{19} counts per revolution or $1.198e-5$ rad/count. Digital torque control of the motor is achieved using a three phase direct drive servo amplifier.

Matlab's xPC target oriented server was used to provide control to the servomechanism drive. For these experiments the digital drive was used in current control mode. This means the output voltage from the 12-bit D/A converter gives a torque command to the actuator's power electronics, which has a time constant of 0.1ms.

The system controller was compiled and run using Matlab's real time xPC Simulink® block code.

2.2 Hybrid PID + Impulse Controller

Figure 3 shows the block diagram of a PID linear controller + impulsive controller. This hybrid controller has been suggested by Li (Li et al., 1998) where the PID driving torque and impulsive controller driving torque are summed together. It is unnecessary to stop at the end of each sampling period; therefore, the controller can be used for both position and speed control.

The controller can be divided into two parts; the upper part is the continuous driving force for large scale movement and control of external force disturbances. The lower part is an additional proportional controller k_{pwm} with a pulse width modulated sampled-data hold (PWMH), and is the basis of the impulsive controller for the control of stick-slip.

The system controller is sampled at 2 kHz. The impulse itself is sampled and applied at one twentieth of the overall sampling period (i.e. 100 Hz) to match the mechanical system dynamics. Figure 4 shows a typical output of the hybrid controller for one impulse sampling period τ_s . The pulse with a height f_p is added to the PID output. Because the PID controller is constantly active, the system has the ability to counteract random disturbances applied to the servomechanism. The continuous part of the controller is tuned to react to large errors and high velocity, while the impulse part is optimized for final positioning where stiction is most prevalent.

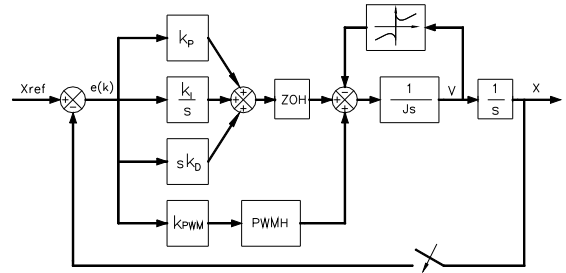


Figure 3: Block diagram of the experimental system controller.

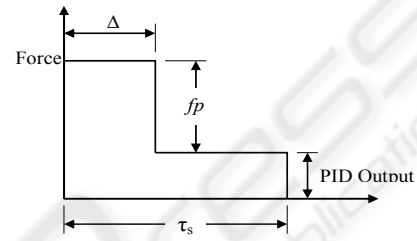


Figure 4: Friction controller output.

For large errors, the impulse width approaches the full sample period τ_s , and for very large errors, it transforms into a continuous driving torque. When this occurs, the combined control action of the PID controller and the impulsive controller will be continuous. Conversely, for small errors, the PID output is too small to have any substantial effect on the servomechanism dynamics.

The high impulse sampling rate, combined with a small error, ensures that the integral (I) part of the PID controller output has insufficient time to rise and produce limit cycling. To counteract this loss of driving torque, when the error is below a threshold, the impulsive controller begins to segment into individual pulses of varying width and becomes the primary driving force. One way of achieving this is to make the pulse width Δ determined by:

$$\Delta = \frac{k_{pwm} \cdot e(k) \tau_s}{f_p} \quad \text{if } k_{pwm} \cdot |e(k)| \leq |f_p|$$

$$\Delta = \tau_s \quad \text{otherwise} \quad (1)$$

In (1)

$$f_p = |f_p| \cdot \text{sign}(e(k)) \quad (2)$$

where $e(k)$ is the error input to the controller, $|f_p|$ is a fixed pulse height greater than the highest static

friction and τ_s is the overall sampling period.

For the experimental results described in this paper, the impulsive sampling period τ_s was 10ms and the pulse width could be incrementally varied by 1ms intervals. The pulse width gain k_{pwm} , is experimentally determined by matching the mechanism's observed displacement d to the calculated pulse width t_p using the equation of motion:

$$d = \frac{f_p(f_p - f_c)}{2mf_c} t_p^2, \quad f_p > 0 \quad (3)$$

The gain is iteratively adjusted until the net displacement for each incremental pulse width is as small as practical.

To further improve the performance of the controller, van Duin (van Duin et al., 2006) use a modified impulse shape to better counteract the dynamics of friction. To overcome stiction, it is necessary to have an initial driving force greater than the static friction. Immediately after motion begins, the opposing friction reduces dramatically and, if motion continues, will be maintained at the Coulomb friction value. Figure 5 shows most of the effective energy of the pulse commences immediately after the static friction dissipates and therefore the remaining pulse height after an initial start-up pulse can be reduced much less than that required to initiate motion.

This type of pulse was used for the experiments in this paper.

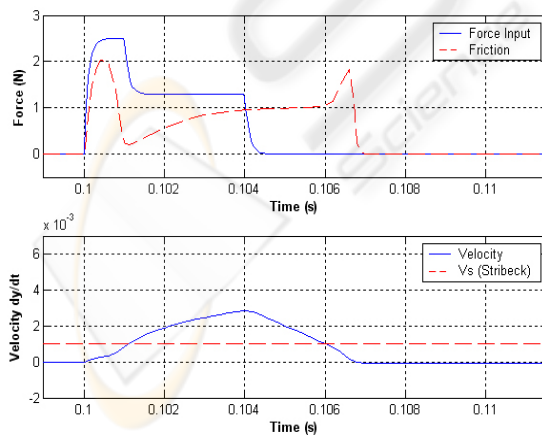


Figure 5: Modified pulse with 2ms start up pulse to overcome static friction and initiate motion.

2.3 Performance at Very Low to High Velocity Regimes

This section investigates how the hybrid PID + impulse controller performs at higher velocities exceeding the Stribeck threshold of approximately .09 rad/s. For this region of velocities, the highly non linear static and negative viscous friction components are substantially reduced relative to the total and the Coulomb and viscous frictions become the dominant resisting friction. For these velocities, the conventional linear PID controller is well suited. Subsequently, the addition of an impulse torque request may be deleterious to the servomechanism's performance in the region of higher velocity.

Figure 6 shows a series of varying ramp responses from 0.02 rad/s up to 0.35 rad/s using the friction test bed. The range of speeds ensures that the mechanism is operating in both the nonlinear and linear friction regions. Figure 7 compares the Mean Value of the Absolute Error (MAE) for each speed from 7 to 10 seconds respectively. A standard form for MAE is (Ogata, 1990):

$$MAE = \frac{1}{n} \sum_{i=1}^n (|x - x_i|) \quad (4)$$

Where n is the number of data points, x_i is the mechanism position, and x is the reference position.

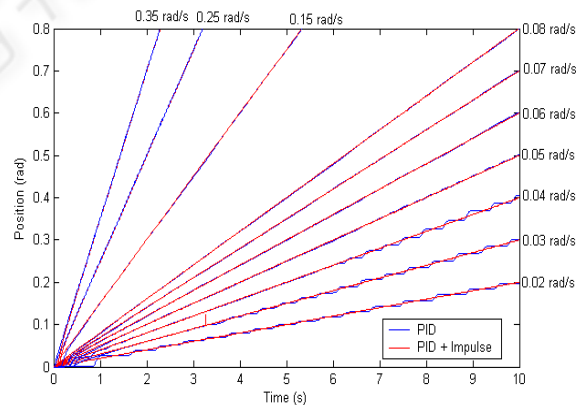


Figure 6: Tracking response for the friction test bed using PID and PID + impulse controllers for varying position ramps (0.02 rad/s to 0.35 rad/s).

For the velocities below the Stribeck velocity threshold, the hybrid PID + impulse controller significantly outperforms the conventional PID controller. However, as the velocity increases, the mean errors of both the PID and PID + impulse controllers begin to converge ($\omega \approx 0.15$ rad/s), and at a

critical velocity above the Stribeck region, the PID controller becomes more precise. This increase in precision for the PID controller can be expected since for this higher range of velocities, a conventional linear PID controller will sufficiently counteract the linear friction without the need of any additional torque. These experiments show that combining the impulse action for high range velocities can be unnecessary and in some instances counterproductive. One way to avoid this loss of performance using a hybrid controller is to disable the impulse torque request at higher velocities to allow the PID part to work autonomously.

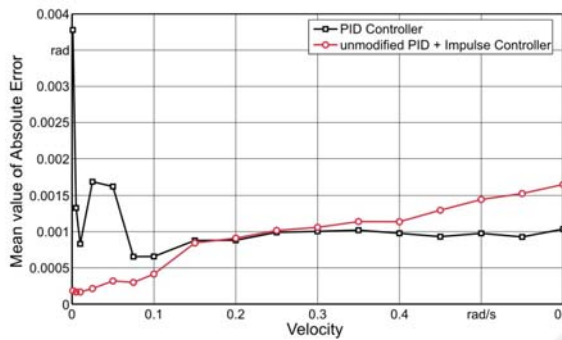


Figure 7: Mean value of the absolute error for each of the position tracking ramps shown in Figure 6 for the period 7 – 10 seconds.

3 TRANSITION VELOCITY CONTROLLER

This section evaluates a series of transition velocity controller functions which disable or limit the impulsive controller above the critical Stribeck velocity.

3.1 On/Off Control using the Critical Velocity

Here the controller's impulsive part is switched off at the critical velocity. The set of conditions for which this occurs is simply defined by the following:

$$\begin{aligned} \text{If } y(v) \leq \text{critical velocity, then the impulse} \\ \text{force } f_p = \text{constant} \\ \text{Otherwise } f_p = \text{zero} \end{aligned} \quad (5)$$

Where $y(v)$ is determined by differentiating the mechanism's actual position.

The initial assumption was that this action would make the system unstable at this moment. Close inspection of a velocity tracking task (Figure 8) confirms the mechanism cyclically overshooting and undershooting. This results in the error of the position tracking task increasing for the critical velocity and velocities nearby. This can be seen in Figure 9 between the velocity range of 0.25 and 0.35 rad/s.

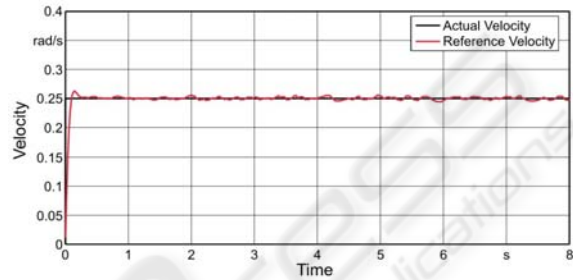


Figure 8: Velocity response when tracking defined disabling velocity of $v=0.25$ rad/s.

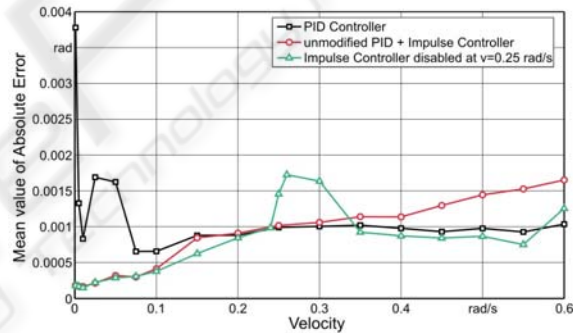


Figure 9: Mean value of the absolute error of the unmodified controllers and the modified PID plus Impulse controller with a disabled impulsive part with respect to the actual velocity.

The loss of torque from the impulsive controller immediately affects the mechanism and the PID controller cannot counteract this quickly enough. The loss of torque causes the velocity to drop under the critical velocity and the impulsive part is immediately enabled again. This makes the system unstable and the controller cyclically enables and disables the impulse controller. However, at velocities above this transition region the position tracking error is consistent with the PID only controller, as expected.

It is clear that using only servomechanism velocity output as a function to control the transition, cannot be an option if tracking accuracies near critical velocities are to be maintained. A solution to this is to transition the controller as a function of

reference velocity rather than system velocity as shown in Figure 10.

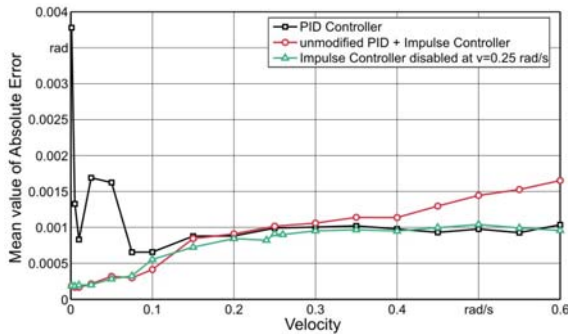


Figure 10: Mean value of the absolute error of the unmodified controllers and the modified PID plus Impulse controller with a disabled impulsive part with respect to the reference velocity.

3.2 Sinusoidal Reference Position Tracking

To further trial the modified controller, an additional experiment tested the system’s ability to track changing velocities that pass through the critical velocity regime. In this case, a sinusoidal position reference ensures a continuous change in velocities for both positive and negative accelerations. By using the Integral Absolute Error (IAE) criterion, the error of a statistically relevant series of position trace experiments can be calculated, and a performance measure between each controller established. A standard measure is given by (Ogata, 1990):

$$\int_0^{\infty} |e(t)| dt \quad (6)$$

Where $e(t)$ is the error with respect to time t .

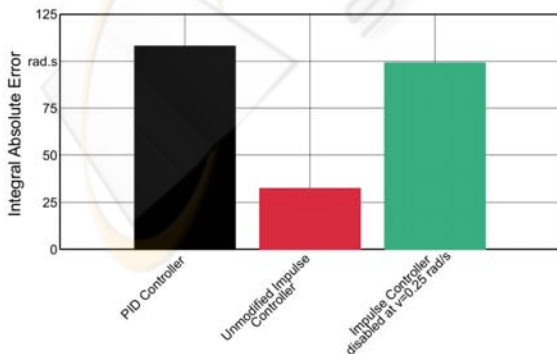


Figure 11: The IAE of the unmodified controllers and the on/off modified controller.

Figure 11 shows a comparison of the results where there is clearly no improvement in accuracy for the modified PID + impulse controller over the original hybrid controller for these conditions of changing velocity. A subsequent breakdown of the error with respect to time shows in Figure 12 that the modified controller mostly counter-performs during acceleration but also partly during deceleration.

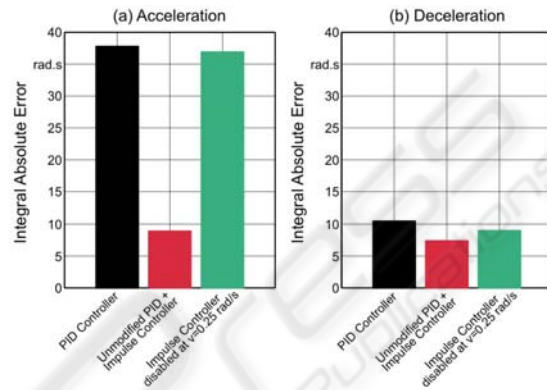


Figure 12: The IAE of the unmodified controllers and the on/off modified controller during (a) acceleration; and (b) deceleration while tracking the sinusoidal position curve.

A closer examination of the position trace (Figure 13) shows that the loss of torque during the point of disabling creates a torque deficiency which the conventional PID controller struggles to correct in a reasonable time frame. A proposed solution to this is to replace the instantaneous on/off switching function with a linear decaying ramp so that abrupt impulse torque removal is avoided and instead gradually transitioned.

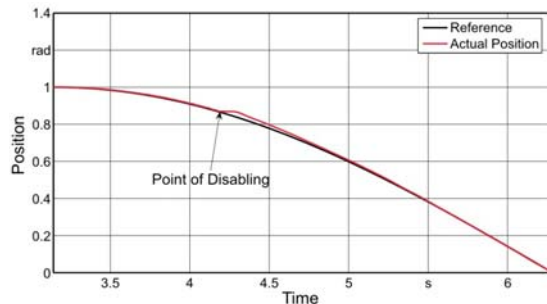


Figure 13: Comparison of the reference and actual position during acceleration while tracking a sinusoidal position input.

3.3 Transition Velocity Function

A solution to transitioning the impulse torque output from unity gain to zero, is given by the following simple linear function:

$$y(v) = a \cdot v + b \quad (7)$$

Where v is the reference velocity of the system and the constants a and b are experimentally determined by trial over a range of velocities either side of the system's critical velocity.

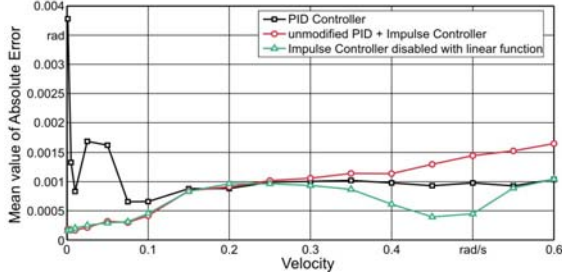


Figure 14: MAE for constant velocity position tracking tasks for the unmodified and linear function transitional impulse controllers.

Figure 14 compares the MAE for each controller. Surprisingly, the linear transition function even improves the accuracy in position at the intermediate higher velocities before the impulse torque is fully transitioned to zero. This improved performance shows that the controller accuracy can be noticeably improved by limiting the pulse height at higher velocities instead of disabling it.

Subsequently, a new function with modified requirements was determined. The function provides:

- A fast reduction in pulse height matched to the PID sampling rate when switching from full to partial impulse control;
- Rather than disabling the full impulse completely it instead reduces it to a fraction of the original pulse height;
- Control over the magnitude of impulse for either acceleration or deceleration regimes.

All of these requirements can be realised with an exponential function. The basic equation used was:

$$y(v) = e^{a(v-b)} + c \quad (8)$$

The parameter a was chosen to be -10 as the exponential function should be designed to have a negative slope that simultaneously reduces the impulse height rapidly. The parameters b and c are determined through boundary conditions as follows:

$$y(v = 0.15) = e^{-10(v-b)} + c = 1 \quad (9)$$

$$y(v = 0.35) = e^{-10(v-b)} + c = 0.25 \quad (10)$$

Solving these equations gives:

$$y(v) = e^{-10(v-0.1358)} + 0.1326 \quad (11)$$

Where v is the reference velocity given by the tracking task. The boundary conditions are selected by trial using a range of varying pulse heights.

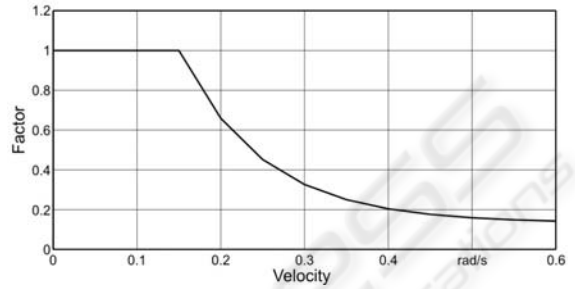


Figure 15: Exponential function for transitioning the limiting of the impulse torque with respect to velocity.

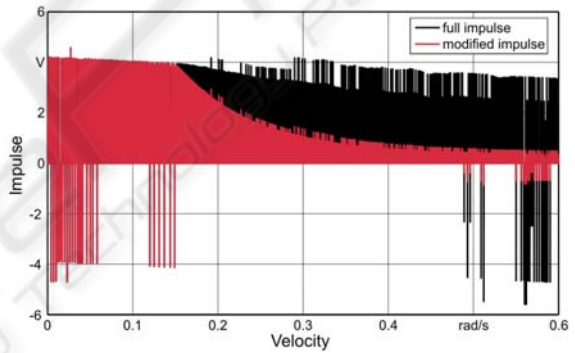


Figure 16: Typical controller torque command for a full impulse and modified impulse applied to friction test bed.

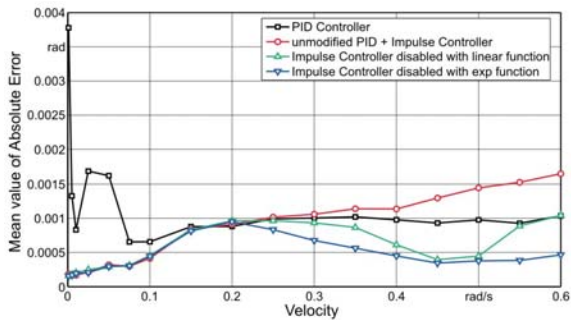


Figure 17: MAE for constant velocity position tracking tasks for the unmodified and transitional impulse controllers.

Figure 15 shows a graphical representation of the exponential function, while Figure 16 gives an example of a typical controller torque command.

The exponential function was shown to provide a significant improvement in the accuracy of velocity tracking (Figure 17). However, further velocity tracking experiments showed that the improvement can only be achieved when tracking constant velocities and is particularly counterproductive during acceleration and varying deceleration. This is caused by the insufficient response of the controller to change the pulse height relative to the rapid changes in velocity.

A solution for ensuring a smooth transition between different tracking tasks with different pulse heights is a time dependant exponential function with additional conditions. If F_1 is the factor determined by the modification done in the previous section, the requirements for the new function are as follows:

$$f(t = 0) = \frac{1}{F_1} \tag{12}$$

$$f(t = \infty) = 1 \tag{13}$$

This leads to the following equation:

$$f(t) = e^{-0.5 \times t + \ln\left(\frac{1}{F_1} - 1\right)} + 1 \tag{14}$$

Multiplying this equation with Equation 11 gives a smooth transition between the full impulse height during the acceleration and the fraction of the pulse height during constant velocity after acceleration. To compare each controller for a range of conditions and to test the controller's stability, a varying position tracking experiment was devised with the resulting trace shown in Figure 18. This trajectory was chosen as a demanding trajectory including several velocity reversals and various velocity gradients.

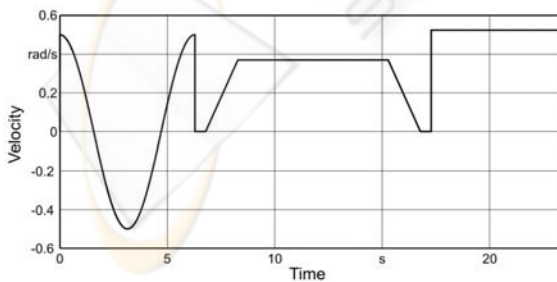


Figure 18: Position tracking task for testing stability.

After repeating the experiments for each controller, the IAE criterion was used to compare

each controller and the results shown in Figure 19. The results clearly show a marked improvement in the overall accuracy of the system when using the impulse controller with a time varying exponential function to transition the impulse torque during acceleration and deceleration. Furthermore, the results show that the controllers are robust enough to remain stable over the fairly demanding range of reference conditions tested.

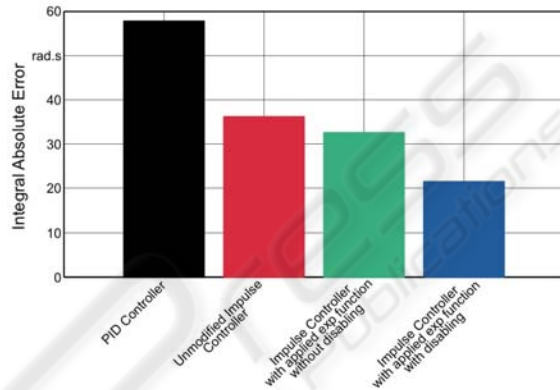


Figure 19: The IAE for the velocity tracking using the unmodified controller, exponential function and exponential function with time varying transition.

3.4 Discussion of Results

This set of results demonstrates the impulse transitional velocity function can be successfully applied to a servomechanism, having characteristics of high non-linear friction. The results show that the unmodified impulse controller significantly outperforms the conventional PID controller at very low velocities. However, as the velocity increases, the mean errors of both the PID and PID + impulse controllers begin to converge above the Stribeck region and the PID controller becomes more precise.

By applying an exponential function which includes consideration of time dependent boundary conditions, the impulse controller can be transitionally reduced to exploit the robustness of a conventional PID controller at higher velocities where viscous friction dominates.

A comparison of the Mean Value of the Absolute Error and the Integral of the Absolute Error for each controller shows that the impulse controller with the velocity dependant exponential function for impulse torque transitioning achieved a more precise result. This controller was proven to be robust enough to maintain stability during a rigorous position tracking task.

4 CONCLUSIONS

Advances in digital control have allowed the power electronics of servo amplifiers to be manipulated in a way that will improve servomechanism precision without modification to the mechanical plant.

A previously developed hybrid PID + Impulse controller which does not require the mechanism to come to a complete stop between pulses has been modified to further improve accuracy in the presence of stick-slip friction. This modification transitions the decay of the impulse torque command at higher velocities. Many experimental tests showed that this innovation provided substantial additional improvement in the mechanism's position accuracy in comparison with other control strategies. This has been demonstrated on a servomechanism which is typical of those used to control each axis of industrial mechanisms such as a robot arm.

Future work is proceeding on optimising the parameters using a method generic to any mechanism, which does not rely on trial and error and is applicable to a greater range of trajectories.

REFERENCES

- Armstrong-Hélouvy, B., 1991, "*Control of Machines with Friction*" Kluwer Academic Publishers, 1991, Norwell MA.
- Armstrong-Hélouvy, B., Dupont, P., and Canudas de Wit, C., 1994, "*A survey of models, analysis tools and compensation methods for the control of machines with friction*" *Automatica*, vol. 30(7), pp. 1083-1138.
- Canudas de Wit, C., Olsson, H., Åström, K. J., 1995 "*A new model for control of systems with friction*" *IEEE Transactions on Automatic Control*, vol. 40 (3), pp. 419-425.
- Dahl, P., 1968, "*A solid friction model*" Aerospace Corp., El Segundo, CA, Tech. Rep. TOR-0158(3107-18)-1.
- Dahl, P., 1977, "*Measurement of solid friction parameters of ball bearings*" Proc. of 6th annual Symp. on Incremental Motion, *Control Systems and Devices*, University of Illinois, ILO.
- Hojjat, Y., and Higuchi, T., 1991 "*Application of electromagnetic impulsive force to precise positioning*" *Int J. Japan Soc. Precision Engineering*, vol. 25 (1), pp. 39-44.
- Johannes, V. I., Green, M.A., and Brockley, C.A., 1973, "*The role of the rate of application of the tangential force in determining the static friction coefficient*", *Wear*, vol. 24, pp. 381-385.
- Johnson, K.L., 1987, "*Contact Mechanics*" Cambridge University Press, Cambridge.
- Kato, S., Yamaguchi, K. and Matsubayashi, T., 1972, "*Some considerations of characteristics of static friction of machine tool slideway*" *J. o Lubrication Technology*, vol. 94 (3), pp. 234-247.
- Li, Z., and Cook, C.D., 1998, "*A PID controller for Machines with Friction*" Proc. Pacific Conference on Manufacturing, Brisbane, Australia, 18-20 August, 1998, pp. 401-406.
- Ogata, K., *Modern Control Engineering*. 1990, Englewood Cliffs, New Jersey: Prentice Hall.
- Olsson, H., 1996, "*Control Systems with Friction*" Department of Automatic Control, Lund University, pp.46-48.
- Popovic, M.R., Gorinevsky, D.M., Goldenberg, A.A., 2000, "*High precision positioning of a mechanism with non linear friction using a fuzzy logic pulse controller*" *IEEE Transactions on Control Systems Technology*, vol. 8 (1) pp. 151-158.
- Rabinowicz, E., 1958, "*The intrinsic variables affecting the stick-slip process*," *Proc. Physical Society of London*, vol. 71 (4), pp.668-675.
- Richardson, R. S. H., and Nolle, H., 1976, "*Surface friction under time dependant loads*" *Wear*, vol. 37 (1), pp.87-101.
- van Duin, S., 2006, "*Impulse Control Systems for Servomechanisms with Nonlinear Friction*", Ph.D. dissertation, University of Wollongong.
- van Duin, S, Cook, C., Li, Z., Alici, G., 2007, "*A modified impulse controller for Improved Accuracy of Robots with Friction*", Proceedings International Conference on Informatics in Control, Automation and Robotics, Angers, France.
- Yang, S., Tomizuka, M., 1988, "*Adaptive pulse width control for precise positioning under the influence of stiction and Coulomb friction*" *ASME J. od Dynamic Systems, Measurement and Control*, vol. 110 (3), pp. 221-227.